Inorg. Chem. **2006**, *45*, 9206–9212

Fluoride Abstraction and Reversible Photochemical Reduction of Cationic Uranyl(VI) Phosphine Oxide Complexes

Shanmugaperumal Kannan, Morgan A. Moody, Charles L. Barnes, and Paul B. Duval*

Department of Chemistry, University of Missouri—Columbia, 601 South College Avenue, Columbia, Missouri 65211

Received May 1, 2006

The syntheses, structural and spectroscopic characterization, fluoride abstraction reactions, and photochemical reactivity of cationic uranyl(VI) phosphine oxide complexes are described. $[UO_2(OPPh_3)_4][X]_2$ (**1a**, X = OTf; **1b**, X = BF_4) and $[UO_2(dppmo)_2(OPPh_3)][X]_2$ (**2a**, X = OTf; **2b**, X = BF_4) are prepared from the corresponding uranyl(VI) chloride precursor and 2 equiv each of AgX and phosphine oxide. The BF_4^- compounds **1b** and **2b** are prone to fluoride abstraction reactions in methanol, leading to dinuclear fluoride-bridged uranyl(VI) complexes. Fluoride abstraction of **2b** in methanol generates two structural isomers of the fluoride-bridged uranyl(VI) dimer $[(UO_2(dppmo)_2)_2(\mu\text{-F})][BF_4]_3$ (**4**), both of which have been structurally characterized. In the major isomer $\mathbf{4^C}$, the four dppmo ligands are all chelating, while in the minor isomer $\mathbf{4^B}$, two of the dppmo ligands bridge adjacent uranyl(VI) centers. Photolysis of **2b** in methanol proceeds through **4** to form the uranium(IV) fluoride complex $[UO_2F_2(dppmo)_3][BF_4]_2$ (**5**), involving another fluoride abstraction step. X-ray crystallography shows **5** to be a rare example of a structurally characterized uranium(IV) complex possessing terminal U–F bonds. Complex **5** reverts to **4** in solution upon exposure to air.

Introduction

The uranyl(VI) ion possesses a long-lived and highly oxidizing excited state as a result of a U 5f ← O 2p ligand-to-metal charge-transfer transition within the robust linear O═U═O group.[1] Among the vast number of organic substrates that are oxidized by the $*UO_2^{2+}$ excited state,[2] primary alcohols reduce uranyl(VI) to uranium(IV) in high quantum yield under anaerobic conditions.[3−5] However, these reactions have typically been conducted in various aqueous (usually acidic) media with minimal attention directed toward the structural and electronic influences of the uranyl(VI) coordination sphere.

We are currently exploring the photochemical reduction of well-defined cationic uranyl(VI) complexes coordinated solely by bulky electron-withdrawing phosphine oxide ligands. From these studies, we have observed that the identity of the counteranion can dramatically influence the photochemical pathway. In this paper, we report how the photoreduction of $[UO_2(dppmo)_2(OPPh_3)][BF_4]_2$ [**2b**; dppmo = $Ph_2P(O)CH_2P(O)Ph_2$] produces the cationic uranium(IV) fluoride complex $[UO_2F_2(dppmo)_3][BF_4]_2$ (**5**), proceeding through *two separate sequences* of fluoride abstraction from BF_4^- anions by a U center. The first occurs prior to photochemical reduction of **2b** and forms the fluoride-bridged dinuclear uranyl(VI) complex $[(UO_2(dppmo)_2)_2(\mu\text{-F})][BF_4]_3$ (**4**), followed by a second fluoride abstraction during photolysis to give **5**. We also note that **5** can be reversibly oxidized to **4** by hydrolysis.

Experimental Section

General Considerations. Unless otherwise stated, all manipulations were conducted under an inert atmosphere of dry, oxygen-free dinitrogen in a MBraun Labmaster 130 glovebox equipped with a MB 20G purification system or in standard Schlenk-type glassware on a dual vacuum/dinitrogen line. Toluene, diethyl ether, and hexanes (Fisher) were dried by passage through an MBraun solvent purification system (MB-SPS) consisting of one column of activated alumina and one column of activated copper catalyst (toluene, hexanes) or two columns of alumina (diethyl ether). Tetrahydrofuran (THF) and dimethoxyethane (DME) were distilled

* To whom correspondence should be addressed. E-mail: duvalP@missouri.edu.

(1) Baird, C. P.; Kemp, T. J. *Prog. React. Kinet.* **1997**, *22*, 87.
(2) Wang, W. D.; Bakac, A.; Espenson, J. H. *Inorg. Chem.* **1995**, *34*, 6034.
(3) Suib, S. L.; Kostapapas, A.; Psaras, D. *J. Am. Chem. Soc.* **1984**, *106*, 1614.
(4) Katsumura, Y.; Abe, H.; Yotsuyanagi, T.; Ishigure, K. *J. Photochem. Photobiol., A* **1989**, *50*, 183.
(5) Nagaishi, R.; Katsumura, Y.; Ishigure, K.; Aoyagi, H.; Yoshida, Z.; Kimura, T.; Kato, Y. *J. Photochem. Photobiol., A* **2002**, *146*, 157.

10.1021/ic060742e CCC: $33.50
Published on Web 10/12/2006

over sodium benzophenone ketyl. Acetonitrile and anhydrous methanol were distilled over CaH_2. Photochemical reactions were conducted with stirring in an Ace Glass reactor assembly operating with output from a 450-W mercury vapor lamp in a quartz immersion well, in an enclosed cabinet. ^{1}H NMR spectra (referenced to a nondeuterated impurity in the solvent) were recorded on a Bruker AMX-250 or -300 spectrometer. ^{31}P{^{1}H} NMR spectra (referenced to external 85% H_3PO_4) were run at 101.25 MHz on the AMX-300 instrument. ^{19}F NMR spectra (referenced to external $CFCl_3$) were run at 235.36 MHz on the AMX-300 instrument. Chemicals shifts are reported in ppm, and all coupling constants are reported in hertz unless otherwise noted. IR spectra were obtained as a mull in a mixture of type NVH and type B immersion oil pressed between KBr plates on a Thermo Nicolet Nexus 670 FT-IR spectrometer. UV/vis spectra were obtained as THF and acetonitrile solutions on a Hewlett-Packard 8452A diode-array spectrophotometer. Elemental analyses were performed by Desert Analytics. Triphenylphosphine oxide, bis(diphenylphospino)-methane (dppm), silver triflate, and silver tetraphenylborate (Aldrich) were used as received. The uranyl complexes $UO_2Cl_2L_2$ (L = *i*-PrC(O)N(*i*-Pr)$_2$),[6] $OPPh_3$,[7] and $OPMePh_2$[7]) were prepared according to literature procedures.

Synthesis of Bis(diphenylphosphino)methane dioxide (dppmo). In a modification of an existing literature preparation,[8] to a solution of dppm (5.0 g, 13 mmol) in 25 mL of benzene was added 2 mL of 50% H_2O_2. The reaction mixture was stirred 2 h, after which the solvent was removed under vacuum and the residue dissolved in 5 mL of methanol. This was added slowly with stirring to 100 mL of water, depositing a white solid that was filtered, washed with water, and dried. The white crystalline product was recrystallized from hot benzene. Yield: 5.0 g (92%).

Synthesis of $[UO_2(OPPh_3)_4][OTf]_2$ (1a). Compound **1a** has been previously reported;[9] the modified preparation described below contrasts with the published procedure in starting from air-stable $UO_2Cl_2(OPPh_3)_2$. Solid $OPPh_3$ (620 mg, 2.23 mmol) and AgOTf (571 mg, 2.23 mmol) were added to a suspension of UO_2Cl_2-$(OPPh_3)_2$ (1.0 g, 1.1 mmol) in CH_2Cl_2 (25 mL), and the reaction mixture was stirred in the dark for 3 h, generating a yellow solution that was filtered. The filtrate was evaporated to dryness, re-extracted with CH_2Cl_2 (5 mL), and filtered a second time to ensure the removal of AgCl, and this filtrate was added to ether (50 mL) with stirring, producing an off-white solid that was filtered, washed with ether, and dried in vacuo. Yield: 1.6 g (85%). The ^{1}H NMR spectrum has been previously reported.[9] ^{31}P{^{1}H} NMR (25 °C, $CDCl_3$): δ 50.3 (s).

Synthesis of $[UO_2(OPPh_3)_4][BF_4]_2$ (1b). This compound was prepared similarly to **1a** using $UO_2Cl_2(OPPh_3)_2$ (1.0 g, 1.46 mmol), solid dppmo (1.22 g, 2.93 mmol), $OPPh_3$ (407 mg, 1.46 mmol), and $AgBF_4$ (572 mg, 2.93 mmol). Yield: 2.0 g (88%). ^{1}H NMR (25 °C, CD_3CN): δ 7.35−7.62 (m, 55H, C_6H_5). ^{31}P{^{1}H} NMR (25 °C, CD_3CN): δ 42.9 (d, $^2J_{PP}$ = 15 Hz, 2P, dppmo), 43.6 (d, $^2J_{PP}$ = 15 Hz, 2P, dppmo), 47.1 (s, 1P, $OPPh_3$). ^{19}F NMR (25 °C, CD_3CN): δ −152.0 (s, BF_4).

Synthesis of $[UO_2(dppmo)_2(OPPh_3)][OTf]_2$ (2a). To a CH_2Cl_2 solution of UO_2Cl_2(*i*-PrC(O)N(*i*-Pr)$_2$)$_2$ (500 mg, 0.73 mmol) were added solid dppmo (610 mg, 1.46 mmol), $OPPh_3$ (204 mg, 0.73 mmol), and AgOTf (377 mg, 1.46 mmol), and the reaction mixture was kept in the dark and stirred for 5 h. The solid AgCl was filtered, and all volatiles were removed in vacuo. The yellow extract was dissolved in 5 mL of CH_2Cl_2 and filtered, and the filtrate was added slowly with stirring to 100 mL of ether. The pale-colored product was filtered, washed with ether, and dried. Compound **2a** was recrystallized from CH_2Cl_2/diethyl ether. Yield: 1.0 g (81%). ^{1}H NMR (25 °C, CD_3CN): δ 4.56 (t, $^2J_{PH}$ = 12 Hz, 4H, PCH_2P), 7.27−7.93 (m, 42H, C_6H_5). ^{31}P{^{1}H} NMR (25 °C, CD_3CN): δ 42.3 (d, $^2J_{PP}$ = 15 Hz, 2P, dppmo), 43.0 (d, $^2J_{PP}$ = 15 Hz, 2P, dppmo), 46.5 (s, 1P, $OPPh_3$). ^{19}F NMR (25 °C, CD_3CN): δ −79.3 (s, CF_3SO_3).

Synthesis of $[UO_2(dppmo)_2(OPPh_3)][BF_4]_2$·DME (2b·DME). This compound was prepared similarly to **2a** using UO_2Cl_2(*i*-PrC-(O)N(*i*-Pr)$_2$)$_2$ (1.0 g, 1.46 mmol), solid dppmo (1.22 g, 2.93 mmol), $OPPh_3$ (407 mg, 1.46 mmol), and $AgBF_4$ (572 mg, 2.93 mmol). The yellow solid was recrystallized from CH_2Cl_2/DME. Yield: 2.0 g (88%). ^{1}H NMR (25 °C, CD_3CN): δ 4.49 (t, $^2J_{PH}$ = 12 Hz, 4H, PCH_2P), 7.27−7.88 (m, 55H, C_6H_5). ^{31}P{^{1}H} NMR (25 °C, CD_3CN): δ 42.9 (d, $^2J_{PP}$ = 15 Hz, 2P, dppmo), 43.6 (d, $^2J_{PP}$ = 15 Hz, 2P, dppmo), 47.1 (s, 1P, $OPPh_3$). ^{19}F NMR (25 °C, CD_3CN): δ −151.9 (s, BF_4).

Synthesis of $[(UO_2(OPMePh_2)_3)_2(\mu$-F)$_2][BF_4]_2$·$2CH_2Cl_2$ (3·$2CH_2Cl_2$). To a suspension of $[UO_2Cl_2(OPMePh_2)_2]$ (500 mg, 0.65 mmol) in CH_2Cl_2 were added $OPMePh_2$ (279 mg, 1.26 mmol) and $AgBF_4$ (252 mg, 1.3 mmol), and the reaction mixture was stirred for 5 h. The solution was filtered to remove AgCl and evaporated to dryness in vacuo. Washing the residue with ether produced a pasty solid. The addition of methanol (5 mL) with stirring deposited a pale-yellow powder that was filtered, washed with ether, and dried. The yellow solid was recrystallized from CH_2Cl_2/DME. Yield: 600 mg (91%). ^{1}H NMR (25 °C, CD_2Cl_2): δ 2.1 (br, 18H, CH_3), 7.37−7.73 (m, 60H, C_6H_5). ^{31}P{^{1}H} NMR (25 °C, CD_2Cl_2): δ 49.9 (s). ^{19}F NMR (25 °C, CD_2Cl_2): δ −153.92 (s, BF_4), −15.1 (s, U−F−U).

Synthesis of $[(UO_2(dppmo)_2)_2(\mu$-F)$][BF_4]_3$ (4). Compound **2b** (500 mg) was dissolved in 25 mL of methanol, and the reaction mixture was stirred for 12 h. The solvent was removed and the residue extracted in 5 mL of CH_2Cl_2 and filtered. The addition of 2 mL of ether to this solution with stirring precipitated a white solid that was filtered, washed with ether, and dried. Recrystallization from CH_2Cl_2/diglyme yielded a mixture of **3** as two separate structural isomers exhibiting distinct crystal habits: a major isomer (70%) as plates and a minor isomer (30%) as needles. Yield (combined): 350 mg (87%).

Major Isomer (**4^C**). ^{1}H NMR (25 °C, CD_3CN): δ 4.29 (t, $^2J_{PH}$ = 12 Hz, 8H, PCH_2P), 7.0−8.0 (m, 80H, C_6H_5). ^{31}P{^{1}H} NMR (25 °C, CD_3CN): δ 40.9 (s). ^{19}F NMR (25 °C, CD_3CN): δ −151.8 (s, BF_4), 32.5 (s, U−F−U). ^{19}F NMR (25 °C, CD_3CN): δ −151.9 (s, BF_4), 107.3 (s, U−F−U).

Minor Isomer (**4^B**). ^{1}H NMR (25 °C, CD_3CN): δ 4.08 (t, $^2J_{PH}$ = 12 Hz, 4H, PCH_2P), 4.26 (t, $^2J_{PH}$ = 12 Hz, 4H, PCH_2P), 6.7−7.5 (m, 80H, C_6H_5). ^{31}P{^{1}H} NMR (25 °C, CD_3CN): δ 43.3 (s), 45.2 (s). ^{19}F NMR (25 °C, CD_3CN): δ −151.8 (s, BF_4), 32.5 (s, U−F−U).

Synthesis of $[UF_2(dppmo)_3][BF_4]_2$ (5). A pale-yellow solution of **2b** (450 mg, 0.33 mmol) in 25 mL of methanol was exposed to UV light for 3 h, and the resulting blue solution was filtered to remove some insoluble yellow material. The addition of ether to the clear filtrate produced a light-blue powder that was filtered, washed with ether, and dried. Recrystallization from CH_3CN/diethyl ether yielded a blue-green crystalline solid. Yield: 212 mg (37%). Compound **5** can also be prepared with the same method starting from **4** (either isomer). ^{1}H NMR (25 °C, CD_3CN): δ −12.7 (br, 6H, PCH_2P), 6.1 (br, 24H, C_6H_5), 6.7 (br t, 12H, C_6H_5), 7.4 (br,

(6) Kannan, S.; Barnes, C. L.; Duval, P. B. *Chem. Commun.* **2005**, 5997.
(7) Arnáiz, F. J. *Inorg. Synth.* **2002**, *33*, 203.
(8) Kannan, S.; Rajalakshmi, N.; Chetty, K. V.; Venugopal, V.; Drew, M. B. G. *Polyhedron* **2004**, *23*, 1527.
(9) Berthet, J.-C.; Nierlich, M.; Ephritikhine, M. *Dalton Trans.* **2004**, 2814.

Table 1. Summary of X-ray Crystallographic Data

	compound			
	2b	**3**	**4^B**	**5**
empirical formula	$C_{72}H_{69}B_2F_8O_9P_5U$	$C_{80}H_{82}B_2Cl_4F_{10}O_{10}P_6U_2$	$C_{101}H_{94}B_2F_{13}O_{14}P_8U_2$	$C_{75}H_{66}B_2F_{10}O_6P_6U$
fw	1644.77	2218.76	2535.01	1698.75
space group	monoclinic, $P2_1/c$	monoclinic, $P2_1/n$	monoclinic, $C2/c$	monoclinic, $P2_1/c$
a, Å	15.0785(12)	13.5921(3)	27.3113(11)	28.0336(12)
b, Å	22.4615(18)	23.7360(6)	17.3101(7)	15.4822(7)
c, Å	20.9624(16)	13.6304(3)	22.2874(9)	18.0718(8)
α, deg	90	90	90	90
β, deg	92.944(1)	93.850(1)	101.515(1)	107.830(1)
γ, deg	90	90	90	90
V, Å^3	7090.3(10)	4387.52(18)	10359.7(7)	7466.8(6)
Z	4	2	4	4
ρ_{calc}, g cm^{-3}	1.541	1.679	1.625	1.511
T, K	173(2)	173(2)	173(2)	173(2)
μ, mm^{-1}	2.479	3.993	3.330	2.378
θ range, deg	1.63−27.15	1.72−27.12	1.40−27.11	1.52−27.14
total no. reflns	49 677	31 089	36 656	52 387
no. of unique reflns	15 605	9626	11 433	16 428
no. of param	884	517	663	901
R1, wR2[a]	0.0323, 0.0767	0.0249, 0.0637	0.0397, 0.0974	0.0517, 0.1079
max, min peaks, e Å^{-3}	1.753, −2.141	0.824, −1.699	0.952, −2.141	0.889, −1.254
GOF	1.035	1.025	1.054	0.966

[a] The value of R1 is based on selected data with $F > 2\sigma(F)$; the value of wR2 is based on all data.

24H, C_6H_5). $^{31}P\{^1H\}$ NMR (25 °C, CD_3CN): δ −81.5 (s). ^{19}F NMR (25 °C, CD_3CN): δ −152 (s, BF_4). Anal. Calcd for $C_{75}H_{66}B_2F_{10}O_6P_6U$: C, 53.03; H, 3.96. Found: C, 52.86; H, 4.26.

X-ray Crystallographic Data. Single crystals of suitable quality for X-ray analysis for **2b**, **3**, **4^B**, and **5** were obtained from the following: layered CH_2Cl_2/DME (**2b** and **3**); layered methanol/diethyl ether (**4^B**); layered CH_3CN/diethyl ether (**5**). Single crystals placed in degassed hydrocarbon oil were mounted on a glass fiber. Intensity data were obtained at −100 °C on a Bruker SMART CCD area detector system using the ω scan technique with Mo Kα radiation from a graphite monochromator. Intensities were corrected for Lorentz and polarization effects. Equivalent reflections were merged, and absorption corrections were made using the multiscan method. Space group, lattice parameters, and other relevant information are given in Table 1. The structures were solved by direct methods with full-matrix least-squares refinement, using the *SHELX* package. All non-hydrogen atoms were refined with anisotropic thermal parameters. The hydrogen atoms were placed at calculated positions and included in the refinement using a riding model, with fixed isotropic U. The final difference map contained no features of chemical significance.

Results and Discussion

Syntheses, Structural Characterization, and Solution Studies of Cationic Uranyl(VI) Phosphine Oxide Complexes. For our purposes of exploring the photochemistry of cationic uranyl(VI) complexes supported exclusively by hard neutral phosphine oxide ligands, we have improved the existing synthetic methodology[8] to chelating phosphine oxides such as dppmo by conducting the oxidation of the precursor bis(phosphine) in benzene rather than in methanol. Following this, a simple metathesis procedure to the uranyl(VI) derivatives $[UO_2(OPPh_3)_2][X]_2$ (**1a**, X = OTf; **1b**, X = BF_4) entails combining $UO_2Cl_2(OPPh_3)_2$ with 2 equiv each of AgX and $OPPh_3$ in CH_2Cl_2, while the syntheses of $[UO_2(dppmo)_2(OPPh_3)][X]_2$ (**2a**, X = OTf;[9] **2b**, X = BF_4) follow a similar method starting from the uranyl(VI) amide adduct $UO_2Cl_2L_2$ [L = (*i*-Pr)C(O)N(*i*-Pr)$_2$][6] and 1 equiv of $OPPh_3$ and 2 equiv each of dppmo and AgX (Scheme 1).[10]

Scheme 1

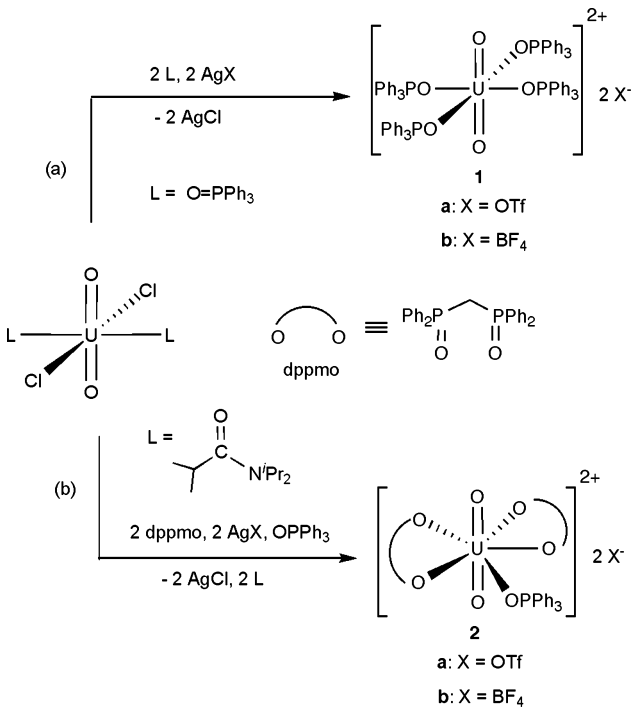

The NMR spectroscopic data for **1a**,**b** reveal a symmetric equatorial coordination environment with a singlet in the respective $^{31}P\{^1H\}$ NMR spectra, matching the structural determination previously obtained for **1a**.[11] Both derivatives of **2** are soluble in CH_2Cl_2 and acetonitrile and insoluble in diethyl ether and hydrocarbon solvents. The $^{31}P\{^1H\}$ NMR spectra of **2a**,**b** in CD_3CN are virtually identical, each

(10) Sarsfield, M. J.; Sutton, A. D.; May, I.; John, G. H.; Sharrad, C. A.; Helliwell, M. *Chem. Commun.* **2004**, 2320.
(11) Berthet, J. C.; Nierlich, M.; Ephritikhine, M. *Angew. Chem., Int. Ed.* **2003**, *42*, 1952.

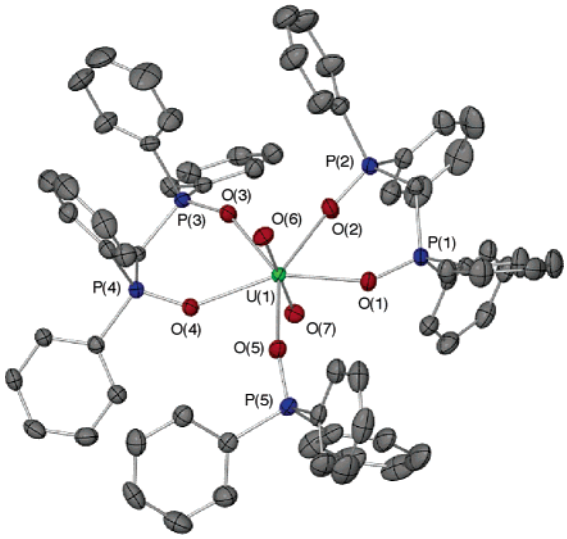

Figure 1. Thermal ellipsoid drawing of the cation of **2b** showing the atom-labeling scheme used in the tables. Displacement ellipsoids are shown at 50% probability.

presenting a singlet near 47 ppm for the $OPPh_3$ ligand and a doublet of doublets at 43 and 44 ppm corresponding to $^2J_{PP}$ coupling between magnetically inequivalent phosphine oxide donors, one residing cis to the $OPPh_3$ ligand and the other trans, belonging to two chemically equivalent dppmo ligands. The corresponding ^{1}H NMR spectra also indicate equivalent phosphine oxides with one triplet ($^2J_{PH} = 12$ Hz) for the dppmo methylene backbone. These spectral data are consistent with the symmetry of the monomeric structure depicted in Scheme 1.

Single crystals suitable for X-ray crystallography were obtained for **2b**. A thermal ellipsoid drawing is shown in Figure 1, and selected bond distances and bond angles are listed in Table 2.

In agreement with the solution NMR data, a seven-coordinate pentagonal-bipyramidal geometry, typical of uranyl(VI) complexes, is observed about the central U atom for the cation of **2b** in the solid state. O atoms from two chelating dppmo ligands and one $OPPh_3$ ligand occupy a relatively ordered equatorial plane (deviation from planarity within 3°) perpendicular to the dioxo group. The structural parameters of the linear O═U═O unit are typical for uranyl-(VI) complexes, while the respective values of U−O bond distances [2.342(2)−2.455(2) Å] and O−U−O chelating bite angles [71.16(8)−71.27(7)°] are similar to those in other structurally characterized uranyl(VI) complexes possessing dppmo ligands, including the other new compounds described here.[8,12,13]

Fluoride Abstraction of Cationic Uranyl(VI) Phosphine Oxide Complexes. Whereas the triflate derivatives **1a** and **2a** remain unaltered in methanol, methanolic solutions of **1b** and **2b** undergo fluoride abstraction from BF_4^- anions in reactions that are likely assisted by strong O−H···F hydrogen-bonding interactions. Similar observations have been reported with other uranyl(VI) complexes containing BF_4^- anions, where the occurrence of fluoride abstraction is limited exclusively to protic solvents.[12] For **1b**, this process forms the known fluoride-bridged species $[(UO_2(OPPh_3)_3)_2(\mu\text{-}F)_2][BF_4]_2$,[12] and the same result occurs in our unsuccessful attempts to isolate $[UO_2(OPMePh_2)_4][BF_4]_2$, which instead yields the corresponding derivative **3** (Scheme 2).

Single crystals suitable for X-ray crystallography were obtained for **3** (Figure 2). Similar to the related $[(UO_2(OPPh_3)_3)_2(\mu\text{-}F)_2][BF_4]_2$,[12] a dimeric structure is observed for the cation in **3**, where each uranyl(VI) unit is coordinated by three terminal phosphine oxide donors and two bridging fluorides, all residing within approximately coplanar pentagonal equatorial coordination geometries. Alignment of the respective dioxo units perpendicular to a shared molecular plane is a common motif in actinide chemistry as exemplified by a number of multinuclear actinyl carbonate compounds.[14] The bridging interactions in **3** are nearly symmetric, with the U(1)−F(1A) bond of 2.3480(17) Å only slightly longer than the U(1)−F(1) bond distance of 2.3122(17) Å. Together with the F(1)−U(1)−F(1A) angle of 64.67(7)°, these bridging parameters are comparable to those in $[(UO_2(OPPh_3)_3)_2(\mu\text{-}F)_2][BF_4]_2$ and related uranyl(VI) complexes.[12] All other structural features in **3** are unremarkable.

The ambient-temperature solution NMR spectroscopic data obtained for **3** do not reflect the solid-state structure. For example, while Figure 2 shows two different $OPMePh_2$ chemical environments in a 2:1 ratio, a broad singlet is observed near 50 ppm in the ^{31}P NMR spectrum while a single broad resonance is seen in the ^{1}H NMR spectrum at 2.1 ppm. These data suggest fluxional phosphine oxide coordination. Cooling a solution of **3** in CD_2Cl_2 to −30 °C resolves the broad resonance in the ^{31}P NMR spectrum into two sharp singlets in a 2:1 ratio at 50.1 and 49.8 ppm, respectively, consistent with the slow-exchange limit for this fluxional process.

Fluoride abstraction in methanol transforms **2b** into the dinuclear complex **4**, which is isolated as a pale-yellow crystalline solid consisting of two separate isomers that possess distinct crystal habits: (1) a major isomer ($\mathbf{4^C}$) as plates; (2) a minor isomer ($\mathbf{4^B}$) as needles (Scheme 3). In repeated experiments, these products were reproducibly obtained in roughly the same 80:20 ratio. Unfortunately, both isomers share similar solubility properties, and thus isolation was limited to manual separation by visual inspection. Nevertheless, the separated materials show individual NMR spectral features that can be identified with, and assigned to, the respective solid-state structure of each isomer (see below), and variable-temperature NMR spectroscopy conducted on a mixture of these isomers reveals no change in the respective ratio as a function of the temperature. These NMR data thus show that the two isomers form separately and do not exist in equilibrium with one another.

Single crystals suitable for X-ray crystallography were obtained for both isomers, although the quality of the crystals

(12) John, G. H.; May, I.; Collison, D.; Helliwell, M. *Polyhedron* **2004**, *23*, 3097.
(13) Sutton, A. D.; John, G. H.; Sarsfield, M. J.; Renshaw, J. G.; May, I.; Martin, L. R.; Selvage, A. J.; Collison, D.; Helliwell, M. *Inorg. Chem.* **2004**, *43*, 5480.
(14) Clark, D. L.; Hobart, D. E.; Neu, M. P. *Chem. Rev.* **1995**, *95*, 25.

Table 2. Bond Lengths (Å) and Angles (deg) for **2b**, **3**, $\mathbf{4^C}$, and **5**

2b		**3**		$\mathbf{4^B}$		**5**	
U(1)−O(1)	2.455(2)	U(1)−O(1)	2.382(2)	U(1)−O(1)	2.361(4)	U(1)−O(1)	2.441(3)
U(1)−O(2)	2.342(2)	U(1)−O(2)	2.368(2)	U(1)−O(2)	2.403(3)	U(1)−O(2)	2.386(4)
U(1)−O(3)	2.385(2)	U(1)−O(3)	2.368(2)	U(1)−O(3)	2.369(3)	U(1)−O(3)	2.465(3)
U(1)−O(4)	2.412(2)	U(1)−O(4)	1.776(2)	U(1)−O(4)	2.363(3)	U(1)−O(4)	2.407(3)
U(1)−O(5)	2.343(2)	U(1)−O(5)	1.773(2)	U(1)−O(5)	1.774(3)	U(1)−O(5)	2.379(3)
U(1)−O(6)	1.762(2)	U(1)−F(1)	2.3122(17)	U(1)−O(6)	1.775(3)	U(1)−O(6)	2.503(3)
U(1)−O(7)	1.760(2)	U(1)−F(1A)	2.3480(17)	U(1)−F(1)	2.3076(14)	U(1)−F(1)	2.123(3)
P=O	1.500(3)−1.511(2)	O=U=O	178.69(10)	P=O	1.492(3)	U(1)−F(2)	2.131(3)
O=U=O	179.35(10)	U(1)−F(1)−U(1A)	115.33(7)	O=U=O	177.94(18)	P=O	1.496(4)−1.516(4)
O(1)−U(1)−O(2)	71.16(8)	F(1)−U(1)−F(1A)	64.67(7)	U(1)−F(1)−U(1A)	134.15(16)	F(1)−U(1)−F(2)	90.07(12)
O(3)−U(1)−O(4)	71.27(7)			O(1)−U(1)−O(2)	72.76(12)	O(1)−U(1)−O(2)	72.17(12)
						O(3)−U(1)−O(4)	74.50(12)
						O(5)−U(1)−O(6)	70.92(12)

Scheme 2

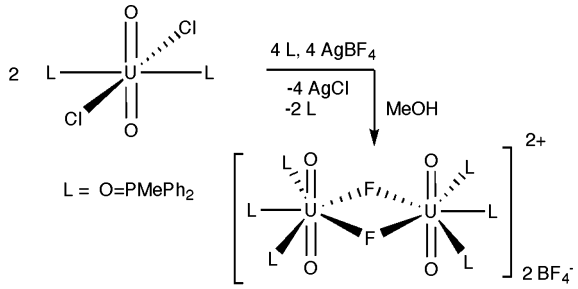

3

of $\mathbf{4^C}$ was insufficient to glean anything beyond connectivity. Each isomer exhibits a dinuclear structure consisting of UO_2-(dppmo)$_2$ units bridged by a single fluoride ligand. Three BF_4^- counterions provide charge balance for two uranyl-(VI) units in each dimeric unit. Thus, the lone compositional change within each uranium coordination sphere from **2b** to **4** consists of replacing the monodentate $OPPh_3$ ligand with a bridging fluoride.

The structural differences between the two isomers $\mathbf{4^C}$ and $\mathbf{4^B}$ can be traced to the different coordination modes adopted

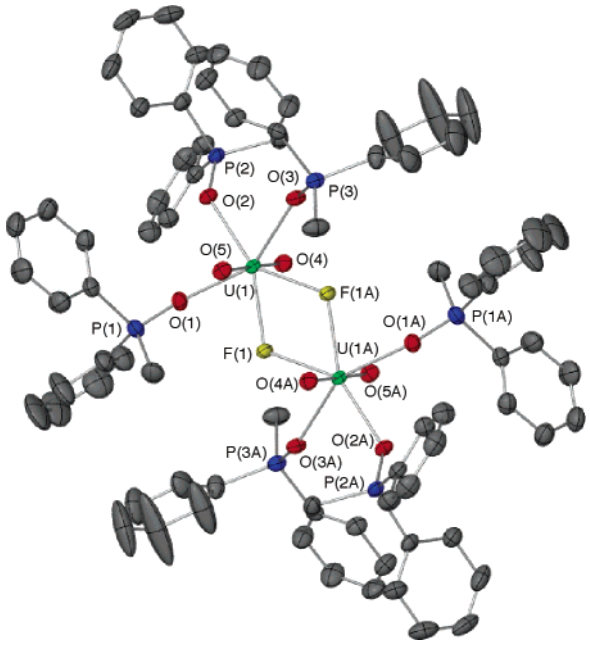

Figure 2. Thermal ellipsoid drawing of the cation of **3** showing the atom-labeling scheme used in the tables. Displacement ellipsoids are shown at 50% probability.

Scheme 3

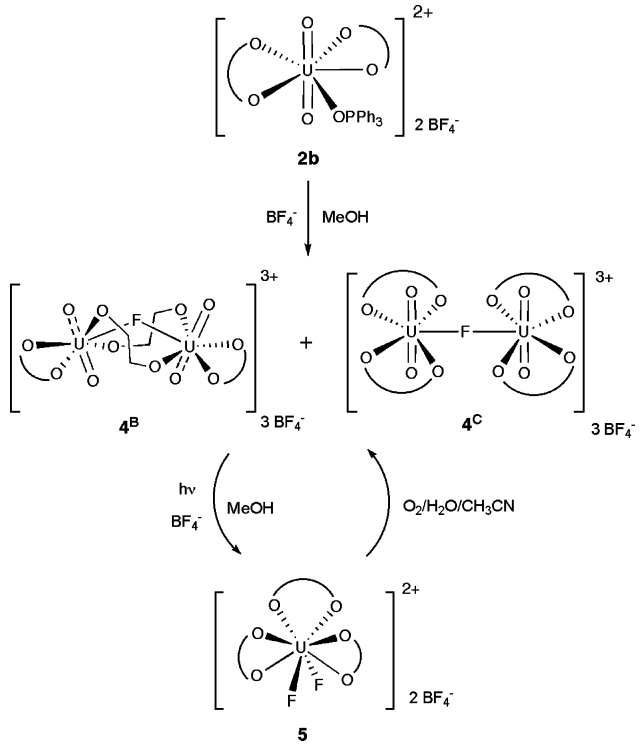

by the dppmo ligands. Whereas each uranyl(VI) center in $\mathbf{4^C}$ is coordinated by two chelating dppmo ligands, thus permitting a normal linear geometry for the U−F−U bridge,[15] one dppmo ligand from each uranyl(VI) unit extends a bridge across to the other metal in $\mathbf{4^B}$ (Figure 3). Bridging is common for dppmo ligands because of the short ligand backbone and has been noted previously for uranyl(VI) derivatives.[8] However, while a single bridging dppmo ligand confers no steric pressure on either uranyl(VI) center,[8] the collective effect of two flanking dppmo bridges in $\mathbf{4^B}$ draws the two U centers in relatively short proximity to one another (approximately 4.2 Å) and squeezes the U(1)−F(1)−U(1A) bridge situated between the dppmo bridges into an unusual bend of 134.15(16)°. This intriguing geometry is reminiscent of A-frame structures adopted by dinuclear dppm-bridged Pt and Pd complexes.[16] Presumably to avoid repulsive

(15) Roussel, P.; Hitchcock, P. B.; Tinker, N.; Scott, P. *Chem. Commun.* **1996**, 2053.
(16) Braun, T.; Steffen, A.; Schorlemer, V.; Neumann, B.; Stammler, H.-G. *Dalton Trans.* **2005**, 3331.

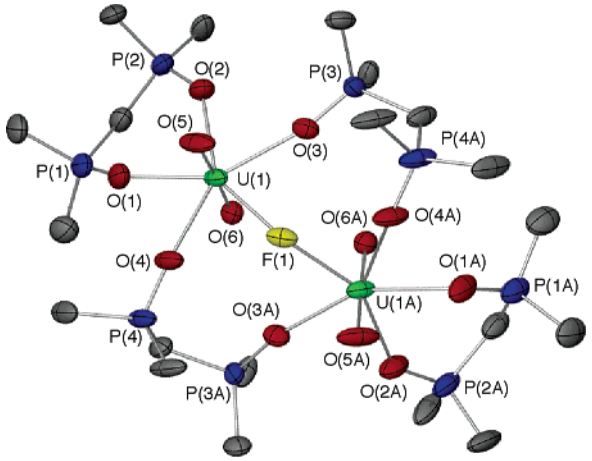

Figure 3. Thermal ellipsoid drawing of the cation of **4**$^{\mathbf{B}}$ showing the atom-labeling scheme used in the tables. Displacement ellipsoids are shown at 50% probability. For clarity, only the *ipso*-C atoms of the phenyl rings are shown.

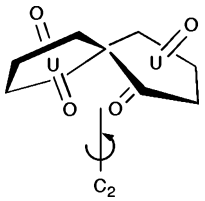

Figure 4. Schematic representation of the staggered conformation of dioxo units in the solid-state structure of **4**$^{\mathbf{B}}$. The bridging fluoride F(1) occupies the shared vertexes of the two pentagonal uranyl(VI) equatorial coordination planes.

electronic interactions between oxo groups that are tilted toward one another as a result of the U−F−U bend, the dioxo groups (and the associated equatorial coordination planes) are twisted approximately 47° with respect to one another into a staggered conformation (Figure 4). Therefore, the only symmetry element in **4**$^{\mathbf{B}}$ is a C_2 axis passing through F(1) that renders the two uranyl(VI) coordination environments equivalent. Despite the unusual geometry, the bridging U(1)−F(1) bond distance of 2.3076(14) Å in **4**$^{\mathbf{B}}$ is similar to those of the bridging U−F bonds in **3**.

NMR spectroscopic data obtained for **4**$^{\mathbf{B}}$ indicate that the solid-state structure is maintained in solution. For example, the ^{1}H and ^{31}P{^{1}H} NMR spectra show separate resonances for the chelating and bridging dppmo ligands, while two singlets are observed at −152 and 32.5 ppm in the ^{19}F NMR spectrum corresponding to the BF_4^- anions and the bridging fluoride, respectively. Chemical shifts for bridging fluorides show a fairly wide range in the compounds described here (−15.1 ppm for **3**, 32.5 ppm for **4**$^{\mathbf{B}}$, and 107.3 ppm for **4**$^{\mathbf{C}}$), with the latter tending toward values (125−135 ppm) found in uranyl(VI) species possessing terminal fluoride ligands.[17]

The situation is slightly different for **4**$^{\mathbf{C}}$, where a singlet in the ^{31}P NMR spectrum (a doublet of doublets similar to that observed for **2** would be anticipated) suggests that a fluxional process analogous to that described for **3** is operative. Cooling a sample of **4**$^{\mathbf{C}}$ to −30 °C yields no change in these spectroscopic features.

(17) Szabó, Z. *Dalton Trans.* **2002**, 4242.

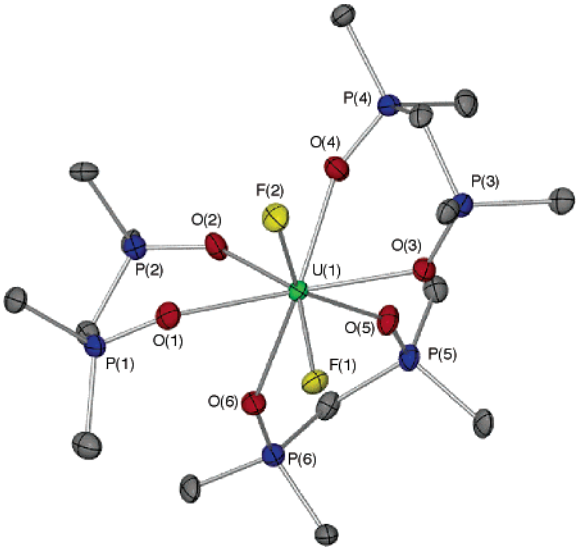

Figure 5. Thermal ellipsoid drawing of the cation of **5** showing the atom-labeling scheme used in the tables. Displacement ellipsoids are shown at 50% probability. For clarity, only the *ipso*-C atoms of the phenyl rings are shown.

Photochemical Reduction of Uranyl(VI) Complexes. Uranyl(VI) complexes have been well documented to undergo photochemical reduction to uranium(IV) with alcohols, although rarely have products been structurally characterized. Such was the case with **1b** and **3**, where a photochemical reduction in methanol produced insoluble bluish-green solids that were not characterized. However, photolysis of **2b** in methanol generates a pale-blue solution within 4 h, from which the uranium(IV) complex **5** can be isolated in good yield as a green crystalline solid after workup in acetonitrile. However, given the facile fluoride abstraction reaction of **2b** in methanol that produces the fluoride-bridged dimer **4**, we also tested the photochemical reactivity of **4** (both isomers together and separately), which again generated **5** in all instances. Therefore, as outlined in Scheme 2, these results suggest that the photochemical transformation from **2b** to **5** proceeds through **4**.

Single crystals suitable for X-ray crystallography were obtained for **5** (Figure 5). Each uranium(IV) center is coordinated by three dppmo ligands and two terminal fluoride donors, thus giving an eight-coordinate geometry that is best described as a distorted dodecahedron,[18] with F(1), O(2), O(3), and O(4) comprising a roughly coplanar trapezoid perpendicular to another trapezoid consisting of F(2), O(1), O(5), and O(6). Allowing for conformational flexibility in the chelating dppmo ligands, the cation in **5** exhibits approximate C_s point group symmetry, with the F−U−F unit defining a mirror plane. The eight-coordinate geometry and three chelating dppmo ligands in **5** resemble the cationic uranium(IV) complex $[U(ReO_4)(dppmo)_3(OH)][ReO_4]_2 \cdot 2CH_3CN$ (**6**).[19]

To the best of our knowledge, the only other structurally characterized uranium(IV) complex possessing a terminal

(18) Hoard, J. L.; Silverton, J. V. *Inorg. Chem.* **1963**, *2*, 235.
(19) John, G. H.; May, I.; Sharrad, C. A.; Sutton, A. D.; Collison, D.; Helliwell, M.; Sarsfield, M. J. *Inorg. Chem.* **2005**, *44*, 7606.

U−F bond is Cp_3UF.[20] The U−F bond distance of 2.106(12) Å in Cp_3UF is comparable to those obtained for **5** [U(1)−F(1) = 2.123(3) Å; U(1)−F(2) = 2.131(3) Å]. The fairly wide range in U−O bond distances in **5** is reflected in alternating short/long distances within individual dppmo ligands. For example, in **5** the shortest and longest U−O bond distances of 2.379(3) and 2.503(3) Å, respectively, are both found with the same dppmo ligand. This feature has been observed in other metal complexes possessing this chelating phosphine oxide ligand.[13,21] Other structural features, including the dppmo O−U−O bite angles [between 70.92(12) and 74.50(12)°], are within the normal range.

In contrast to the relatively soluble fluoride-bridged uranyl(VI) species **3** and **4**, compound **5** is soluble only in acetonitrile with prolonged heating and/or stirring. The $^{31}P\{^1H\}$ NMR spectrum of **5** in CD_3CN shows a sharp singlet at −81.5 ppm, while a paramagnetically shifted and broadened resonance at −12.7 ppm is observed for the methylene dppmo backbone in the ^1H NMR spectrum, both indicating an averaged chemical environment for all three dppmo ligands. Resonances are not seen for the terminal fluoride ligands in the corresponding ^{19}F NMR spectrum, however, presumably because they are directly bound to the paramagnetic uranium(IV) center. Spectra acquired at elevated temperatures also presented no observable resonances. The f^2 center may also be responsible for the significant upfield shift of the ^{31}P NMR resonance for the coordinated dppmo ligands in **5** relative to that of the free ligand near 22 ppm. However, it should be noted that the chelating dppmo ligands in the related uranium(IV) species **6** exhibit *downfield* chemical shifts near 40 ppm in the ^{31}P NMR spectrum.[19] In this context, we cannot rationalize the contrasting upfield shift seen in **5**.

Uranyl(VI) reduction, proceeding either photochemically or through the use of appropriate reducing agents, is typically accompanied by significant changes in the uranium coordination sphere.[1,22] In both instances, this arises from enhanced lability of the uranyl(V) intermediate[23] and accounts for the structural rearrangement observed here, whereby the dioxo group in the precursor **4** is replaced by additional fluoride and dppmo ligands in **5**. On the basis of the stoichiometry of three dppmo and two fluoride ligands in **5**, a theoretical yield of 67% (based on U) is set by the limited availability of two dppmo units from each U center in the precursor **4**. Similarly, the single bridging fluoride in dinuclear **4** would normally limit the theoretical yield further to 25% (to furnish two fluorides in **5**), so the actual isolated yield of 36% necessitates further abstraction of at least an additional 1 equiv of BF_4^- during the photochemical reduction.

Although green crystalline samples of **5** remain air-stable indefinitely (i.e., months) in the solid state, an acetonitrile solution of **5** turns yellow over the course of 1 day upon the addition of a few drops of water (with O_2 serving as the probable oxidant, although no reaction is observed when dry O_2 is added instead), eventually regenerating both isomers of the uranyl(VI) fluoride-bridged dimer **4** in approximately the same ratio as that obtained through fluoride abstraction from **2b**. This result illustrates an equal degree of lability associated with uranium(IV) oxidation as is found with uranyl(VI) reduction, presumably because both proceed through the same reactive uranyl(V) intermediate. These observations also suggest considerable kinetic and/or thermodynamic stability of **4**, whereby two different reaction pathways converge at the same product.

Conclusions

The results described here illustrate how the identity of the anion can have an important impact upon the photochemistry of cationic uranyl(VI) complexes. For example, in the photoreduction of **2b** with methanol, we have observed two sequences of fluoride abstraction from BF_4^-, one prior to photochemical reduction and the other during. We are continuing our investigation into the effects of the equatorial coordination sphere, solvent, and counterions in the photochemical reduction of uranyl(VI) species.

Acknowledgment. The American Chemical Society Petroleum Research Fund, the Missouri University Research Reactor, and the University of Missouri Research Board are acknowledged for partial financial support of this work.

Supporting Information Available: X-ray crystallographic files in CIF format for **2b**, **3**, **4^B**, and **5** and ^1H and ^{31}P NMR spectra for **1b**, **2a**,**b**, **3**, and **4** (as evidence for purity). This material is available free of charge via the Internet at http://pubs.acs.org.

IC060742E

(20) Ryan, R. R.; Penneman, R. A.; Kanellapulos, B. *J. Am. Chem. Soc.* **1975**, *97*, 4258.
(21) Bermejo, E.; Castineiras, R.; Dominguez, R. *J. Coord. Chem.* **1994**, *33*, 353.
(22) Greiwing, H.; Krebs, B.; Pinkerton, A. A. *Inorg. Chim. Acta* **1995**, *234*, 127.
(23) Selbin, J.; Ortego, J. D. *Chem. Rev.* **1969**, *69*, 657.